

## PERFORMANCE-BASED EVALUATION OF LATERAL SPREADING DISPLACEMENT

Steven L. KRAMER<sup>1</sup>, Kevin W. FRANKE<sup>2</sup>, Yi-Min HUANG<sup>3</sup>, David A. BASKA<sup>4</sup>

### ABSTRACT

Liquefaction-induced lateral spreading poses a significant hazard to bridges, lifelines, buildings and other elements of the built environment. At a given site, lateral spreading can be caused by ground motions from multiple sources, and from earthquakes of different magnitudes produced by each source; therefore, lateral spreading can be caused by ground motions with a wide range of return periods. While conventional lateral spreading evaluation procedures focus on loading scenarios associated with a particular return period, a performance-based procedure allows consideration of loading from all return periods.

This paper describes a procedure for evaluation of liquefaction-induced lateral spreading displacement. The procedure uses a probabilistic, empirical lateral spreading model modified to fit within the framework of a conventional probabilistic seismic hazard analysis. The procedure allows calculation of hazard curves for lateral spreading displacement conditional upon site conditions (i.e. SPT resistance profile, ground slope or free-face ratio); the hazard curves can be used, with the standard Poisson assumption, to compute probabilities of lateral spreading displacement exceedance within a given exposure period.

Keywords: Liquefaction, lateral spreading, deformation, performance, hazard analysis

### INTRODUCTION

Liquefaction-induced lateral spreading has caused substantial damage to buildings, bridges, embankments, buried utilities, and other constructed facilities in numerous past earthquakes. Protection of such elements of modern infrastructure requires that the potential for lateral spreading be carefully considered in the design of new structures and in evaluations of the safety of existing structures. Because much of the damage associated with soil liquefaction is related to deformations, accurate prediction of anticipated lateral spreading displacement is required for both design and evaluation procedures. Although significant advances in understanding the mechanics of liquefaction and lateral spreading have been made in recent years, available procedures for *a priori* prediction of lateral spreading displacement remain empirical in nature. Furthermore, the relative paucity of well-documented lateral spreading case histories leads to considerable scatter in the data from which these

---

<sup>1</sup>John R. Kiely Professor of Civil Engineering, University of Washington, Seattle, WA Email: [kramer@u.washington.edu](mailto:kramer@u.washington.edu)

<sup>2</sup>Staff Geotechnical Engineer, Kleinfelder Associates, Boise, ID, formerly Graduate Student, University of Washington, Seattle, WA, Email: [kfranke@kleinfelder.com](mailto:kfranke@kleinfelder.com)

<sup>3</sup>Graduate student, University of Washington, Seattle, WA Email: [ninerh@u.washington.edu](mailto:ninerh@u.washington.edu)

<sup>4</sup>Senior engineer, Terracon, Inc., Seattle WA Email: [dabaska@terracon.com](mailto:dabaska@terracon.com)

empirical procedures are developed. As a result, the lateral spreading displacements estimated by these empirical procedures have a significant level of uncertainty.

Performance-based earthquake engineering seeks to provide more rational, complete, and accurate estimates of earthquake losses by integrating the prediction of ground motion, response, physical damage, and losses with consideration of the uncertainties in each and in the relationships between them. By accounting for the significant uncertainties in both ground motions and response, the performance-based approach is particularly well-suited to the problem of estimating hazards from lateral spreading displacements.

## LATERAL SPREADING

Lateral spreading refers to the accumulation of permanent lateral displacement in soils subjected to earthquake shaking in the presence of static driving stresses. Lateral spreading has been observed in numerous earthquakes. Among the best-known examples are those in Niigata, Japan and Anchorage, Alaska. More recently, significant lateral spreads have been observed in California (Boulanger et al., 1997; Holzer, 1998), Japan (Comartin et al., 1995; Hamada and Wakamatsu, 1998), and Turkey (Bardet et al., 2000; Cetin et al., 2004). Field evidence of lateral spreading generally includes ground cracking (with and without sand boils) with permanent displacement in the downslope direction or toward nearby free slopes. The ground surface displacements caused by lateral spreading can be measured by surveying methods (given that a pre-earthquake survey exists) or by air photo interpretation.

## ESTIMATION OF LATERAL SPREADING DISPLACEMENT

Several investigators have developed predictive relationships for the permanent displacement produced by lateral spreading. Early models (e.g. Hamada et al., 1987; Youd and Perkins, 1987) and some later models (e.g. Rauch and Martin, 2000) considered some of the variables known to influence lateral spreading displacements. More recent models commonly used in practice, however, consider the influence of soil properties, slope geometry, and level of ground motion, though they represent them in different ways.

Bartlett and Youd (1992) compiled a large database of lateral spreading case histories from Japan and the western United States. By investigating a large number of potential parameters, Bartlett and Youd (1992) were able to identify those that were most closely related to lateral spreading displacement and develop a regression-based predictive relationship. Youd et al. (2002) used an expanded and corrected version of the 1992 database to develop the predictive relationship

$$\log D_H = b_0 + b_1 M_w + b_2 \log R^* + b_3 R + b_4 \log W + b_5 \log S + b_6 \log T_{15} + b_7 \log(100 - F_{15}) + b_8 \log(D50_{15} + 0.1 \text{ mm}) \quad (1)$$

where  $D_H$  = horizontal displacement in meters,  $M_w$  = moment magnitude,  $R^* = R + 10^{-0.89M_w - 5.64}$ ,  $R$  = closest horizontal distance to the energy source,  $W$  = free-face ratio (Figure 4) in percent,  $S$  = ground slope in percent,  $T_{15}$  = cumulative thickness (in upper 20 m) of saturated cohesionless soil with  $(N_1)_{60} < 15$  (subject to the restriction that the top of the layer is at a depth of 1 to 10 m),  $F_{15}$  = average fines content of the soil comprising  $T_{15}$ , and  $D50_{15}$  = average mean grain size (mm) of the soil comprising  $T_{15}$ . The values of the coefficients are presented in Table 1.

**Table 1. Coefficients for Youd et al. (2002) model.**

Model	$b_0$	$b_1$	$b_2$	$b_3$	$b_4$	$b_5$	$b_6$	$b_7$	$b_8$
Ground slope	-16.213	1.532	-1.406	-0.012	0	0.338	0.540	3.413	-0.795
Free Face	-16.713	1.532	-1.406	-0.012	0.592	0	0.540	3.413	-0.795

The concept of density-related potential strains and its role in estimating liquefaction-related deformations (e.g. Seed et al, 1973; Seed et al., 1975; Seed, 1979) was developed many years ago. In

recent years, new models for estimating lateral spreading displacements based on strain potential (e.g. Shamoto et al., 1998; Zhang et al., 2004; Faris et al., 2006) have been proposed. For example, Zhang et al. (2004) capped the laboratory test-based maximum cyclic shear strains predicted as a function of relative density and factor of safety against liquefaction by Ishihara and Yoshimine (1992) with the limiting shear strains proposed by Seed (1979) to develop a cumulative shear strain-based model for lateral spreading displacement. Using empirical relationships between penetration resistance and relative density, either SPT or CPT data can be used to predict permanent displacements as

$$D_H = \begin{cases} (S + 0.2) \cdot LDI & \text{ground slope case} \\ 6W^{-0.8} \cdot LDI & \text{free - face case} \end{cases} \quad (2)$$

both with the lateral displacement index,  $LDI$ , computed by integrating maximum cyclic shear strain,  $\gamma_{\max}$ , over depth, i.e.

$$LDI = \int_0^{Z_{\max}} \gamma_{\max} dz \quad (3)$$

where  $Z_{\max}$  = maximum depth below all potentially liquefiable layers with  $FS < 2.0$ .

Baska (2002) used a series of numerical analyses with a nonlinear model capable of representing the response of sloping deposits of liquefiable soil to identify an appropriate form for a predictive model. Baska then calibrated that model against a database of lateral spreading case histories, thereby producing a model that was consistent with the mechanics of liquefiable soil behavior, nonlinear site response, and observed lateral spreading behavior. The Baska model produces a smooth transition in displacement with respect to SPT resistance, accounts for the effects of layer depth on displacement, and allows estimation of the uncertainty in predicted displacement. The Baska model computes the median lateral spreading displacement as

$$\hat{D}_H = \begin{cases} 0 & \text{for } \sqrt{D_H} \leq 0 \\ (\sqrt{D_H})^2 & \text{for } \sqrt{D_H} > 0 \end{cases} \quad (4)$$

where

$$\sqrt{D_H} = \frac{\beta_1 + \beta_2 T_{gs}^* + \beta_3 T_{ff}^* + 1.231M - 1.151 \log R^* - 0.01R + \beta_4 \sqrt{S} + \beta_5 \log W}{1 + 0.0223(\beta_2 / T_{gs}^*)^2 + 0.0135(\beta_3 / T_{ff}^*)^2} \quad (5)$$

$$T_{gs}^* = 2.586 \sum_{i=1}^n t_i \exp[-0.05N_i - 0.04z_i] / [1 + (PI_i / 5.5)^8]$$

$$T_{ff}^* = 5.474 \sum_{i=1}^n t_i \exp[-0.08N_i - 0.10z_i] / [1 + (PI_i / 5.5)^8]$$

$$R^* = R + 10^{(0.89M - 5.64)}$$

$z$  = depth in meters,  $PI$  = plasticity index, and the regression parameters are as indicated in Table 2. It should be noted that the Baska (2002) model, unlike the Youd et al. (2002) model, predicts zero lateral spreading displacement for some conditions (e.g. low magnitude and/or large distance events).

**Table 2. Coefficients for Baska (2002) model.**

Model	$\beta_1$	$\beta_2$	$\beta_3$	$\beta_4$	$\beta_5$
Ground slope	-7.207	0.067	0.0	0.544	0.0
Free face	-7.518	0.0	0.086	0.0	1.007

The level of agreement between observed and median predicted displacements is shown in Figure 1; the  $R^2$  value of 0.849 is only slightly higher than that (0.836) reported by Youd et al. (2002). The square root transformation of  $D_H$  was found to produce residuals that were approximately normally distributed with constant variance,  $\sigma_{\sqrt{D_H}}^2 = 0.0784$ . The probability of exceeding some non-negative lateral spreading displacement,  $d$ , can therefore be estimated as

$$P[D_H > d] = 1 - \Phi \left[ \frac{\sqrt{d} - \sqrt{D_H}}{\sigma_{\sqrt{D_H}}} \right] \quad (6)$$

where  $\Phi$  is the standard normal cumulative distribution. It should be noted that negative values of  $\sqrt{D_H}$ , which can occur for some combinations of input parameters (e.g. low magnitudes and/or large distances), can be used to compute exceedance probabilities.

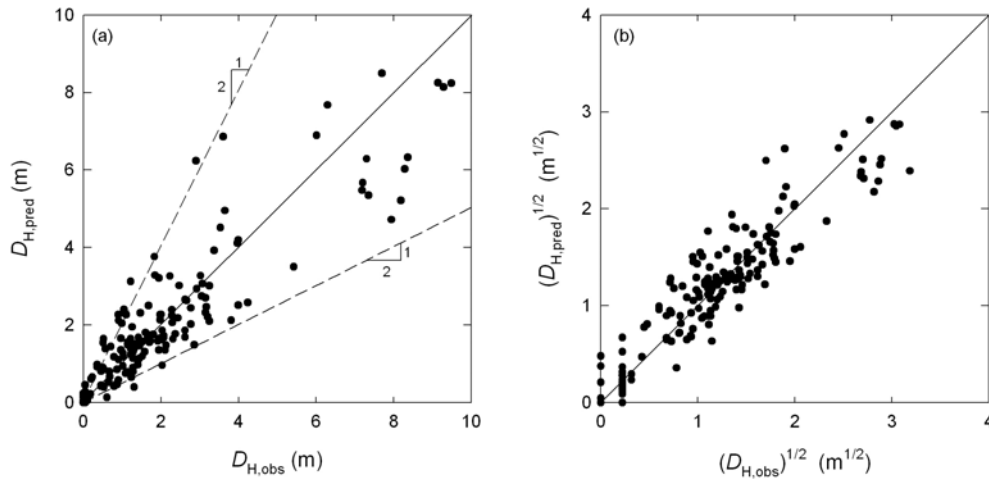


**Figure 1. Relationship between predicted median and observed lateral spreading displacements using Baska (2002) model: (a) natural scale, and (b) transformed scale.**

### PROBABILISTIC SEISMIC HAZARD ANALYSIS

Ground shaking levels used in seismic design and hazard evaluations are generally determined by means of seismic hazard analyses. Deterministic seismic hazard analyses are used most often for special structures or for estimation of upper bound ground shaking levels. In the majority of cases, however, ground shaking levels are determined by probabilistic seismic hazard analyses. Probabilistic seismic hazard analyses (PSHA) consider the potential levels of ground shaking from all combinations of magnitude and distance for all known sources capable of producing significant shaking at a site of interest. The distributions of magnitude and distance, and of ground shaking level conditional upon magnitude and distance, are combined in a way that allows estimation of the mean annual rate at which a particular level of ground shaking will be exceeded. The mean annual rate of exceeding a ground motion parameter value,  $y$ , can be computed as

$$\lambda_y = \sum_{i=1}^{N_S} v_i \sum_{j=1}^{N_M} \sum_{k=1}^{N_R} P[Y > y | M = m_j, R = r_k] P[M = m_j] P[R = r_k] \quad (7)$$

where  $N_S$ ,  $N_M$ , and  $N_R$  are the number of seismic sources, discretized magnitudes, and discretized source-site distances, respectively, and  $v_i$  is the mean annual rate of exceedance of some minimum magnitude for the  $i^{\text{th}}$  source. The reciprocal of the mean annual rate of exceedance is commonly referred to as the return period. The results of a PSHA are typically presented in the form of a seismic hazard curve, which graphically illustrates the relationship between  $\lambda_y$  and  $y$ . In Equation (5), the conditional probability expression is typically obtained from a ground motion attenuation relationship.

## PERFORMANCE-BASED FRAMEWORK FOR LATERAL SPREADING DISPLACEMENT

In practice, lateral spreading displacements are usually evaluated using a deterministic lateral spreading model and a single scenario corresponding to a single ground motion hazard level, for example, for ground motions with a 475-yr return period. In contrast, a performance-based approach incorporates a probabilistic lateral spreading model and contributions from *all* possible earthquake scenarios.

PBEE is generally formulated in a probabilistic framework to evaluate the risk associated with earthquake shaking at a particular site. The risk can be expressed in terms of economic loss, fatalities, or other measures. The Pacific Earthquake Engineering Research Center (PEER) has developed a probabilistic framework for PBEE (Cornell and Krawinkler, 2000; Krawinkler, 2002; Deierlein et al., 2003) that computes risk as a function of ground shaking through the use of several intermediate variables. The ground motion is characterized by an *Intensity Measure*, *IM*, which could be any one of a number of ground motion parameters (e.g.  $a_{\max}$ , Arias intensity, etc.). The effects of the *IM* on a system of interest are expressed in terms used primarily by engineers in the form of *Engineering Demand Parameters*, or *EDPs* (e.g. excess pore pressure, permanent displacement, etc.). The physical effects associated with the *EDPs* (e.g. settlement, cracking, etc.) are expressed in terms of *Damage Measures*, or *DMs*. Finally, the risk associated with the *DM* is expressed in a form that is useful to decision-makers by means of *Decision Variables*, *DV* (e.g. repair cost, downtime, etc.). The mean annual rate of exceedance of various *DV* levels,  $\lambda_{DV}$ , can be expressed in terms of the other variables as

$$\lambda_{dv} = \sum_{k=1}^{N_{DM}} \sum_{j=1}^{N_{EDP}} \sum_{i=1}^{N_{IM}} P[DV > dv | DM = dm_k] P[DM = dm_k | EDP = edp_j] P[EDP = edp_j | IM = im_i] \Delta \lambda_{im_i} \quad (8)$$

where  $P[a|b]$  describes the conditional probability of  $a$  given  $b$ , and  $N_{DM}$ ,  $N_{EDP}$ , and  $N_{IM}$  are the number of increments of *DM*, *EDP*, and *IM*, respectively. Extending this approach to consider epistemic uncertainty in *IM*, although not pursued in this paper, is straightforward. By integrating over the entire hazard curve (approximated by the summation over  $i = 1, N_{IM}$ ), the performance-based approach includes contributions from all return periods, not just the return periods mandated by various codes or regulations.

The portion of the performance-based process that geotechnical engineers are most commonly involved with is the estimation of response expressed by the *EDP*. This process can be extracted from Equation (8) and formulated in terms of the mean annual rate of *EDP* exceedance, i.e. as

$$\lambda_{edp} = \sum_{i=1}^{N_{IM}} P[EDP > edp | IM = im_i] \Delta \lambda_{im_i} \quad (9)$$

### Alternate Form of Baska Model

As indicated above, development of a performance-based lateral spreading procedure requires a lateral spreading model capable of predicting the probability distribution of lateral spreading displacement. As a result, deterministic models such as the previously described Youd et al. (2002) and Zhang et al.

(2004) models, are not suitable for performance-based analyses. The form of the Baska (2002) lateral spreading model, however, is well-suited for development of a performance-based lateral spreading procedure.

Consider the Baska (2002) lateral spreading model for ground slope cases. The terms on the right side of Equation (5) can be grouped into those associated with loading, site conditions, and uncertainty, thereby allowing the relationship to be written as

$$\sqrt{D_H} = \mathcal{L} + \mathcal{S} + \varepsilon \quad (10)$$

where the loading, site, and uncertainty terms are respectively defined as

$$\mathcal{L} = 1.231M - 1.151 \log R^* - 0.01R$$

$$\mathcal{S} = \beta_1 + \beta_2 T_{gs}^* + \beta_3 T_{ff}^* + \beta_4 \sqrt{S} + \beta_5 \log W$$

$$\varepsilon = \sigma_{\sqrt{D_H}} \Phi^{-1}[P]$$

and  $P$  is the probability of exceeding the lateral spreading displacement,  $D_H$ . The loading term is a function of magnitude and distance, as are typical attenuation relationships. In fact, the expression for the loading term can be interpreted as an attenuation relationship for Baska's loading parameter,  $\mathcal{L}$ . The relationship is shown graphically in Figure 2.

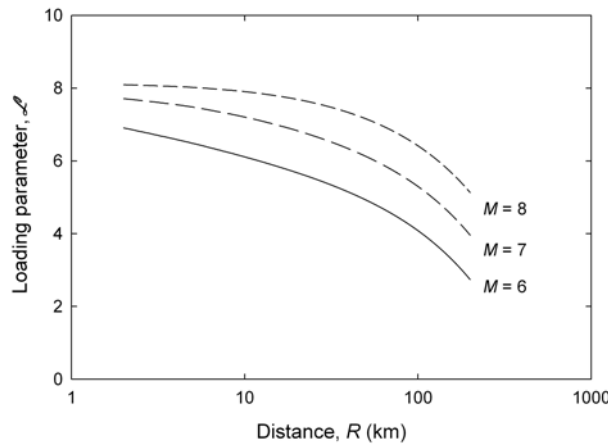


**Figure 2. Variation of loading parameter,  $\mathcal{L}$ , with magnitude and distance.**

The probability of exceeding some lateral spreading displacement level,  $d$ , is illustrated schematically in Figure 3. From Equation 10, lateral spreading displacement increases linearly with  $\mathcal{L}$ , so the relationship between median displacement and  $\mathcal{L}$  has unit slope and an intercept that depends on the site parameter,  $\mathcal{S}$ , i.e., on material properties (SPT resistance) and geometry (depth of liquefiable soils and ground slope). However, the square root transformation can lead, as illustrated by the probability distribution shown in Figure 3, to some finite probability of negative values of  $\sqrt{D_H}$ , which represent the probabilities of zero displacement. Given Baska's constant value of  $\sigma_{\sqrt{D_H}} = 0.28$ , the probability of zero displacement depends on the size of the intercept and the value of  $\mathcal{L}$ . If the intercept is small (thin/dense liquefiable layers and/or flat slope) and the loading is low (low  $M$  and/or high  $R$ ), the probability of zero displacement will be high. The combination of  $M$  and  $R$  values at which the Baska (2002) model predicts zero displacement corresponds well to the bounding conditions for field observations of liquefaction reported by Ambraseys (1988).

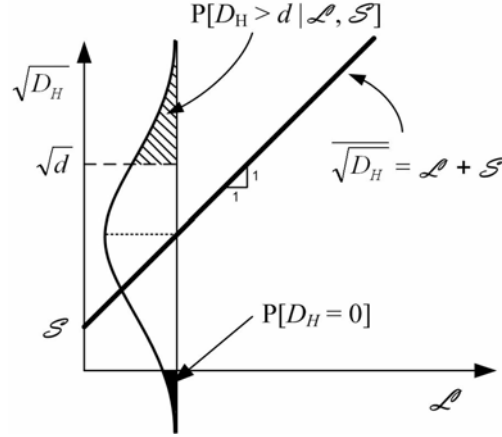


Figure 3. Schematic illustration of variation of  $\sqrt{D_H}$  with  $\mathcal{L}$  and  $\mathcal{S}$  for Baska model.

### Performance-Based Implementation of Baska Model

Using the alternative formulation of the Baska (2002) model, a performance-based lateral spreading model can be expressed (assuming a single source for simplicity) in terms of lateral spreading displacement conditional upon the site term, i.e. as

$$\lambda_{d|\mathcal{S}} = \sum_{i=1}^{N_L} P[D_H > d | \mathcal{S}, \mathcal{L}_i] \Delta \lambda_{\mathcal{L}_i} \quad (11)$$

which, introducing the mean annual rate of exceedance of a minimum event of interest,  $\nu$ , can also be written as

$$\lambda_{d|\mathcal{S}} = \nu \sum_{i=1}^{N_L} P[D_H > d | \mathcal{S}, \mathcal{L}_i] P[\mathcal{L}_i] \quad (12)$$

Recognizing that  $\mathcal{L} = f(M, R)$  and making the usual assumption of independence of  $M$  and  $R$ , then

$$\lambda_{d|\mathcal{S}} = \nu \sum_{j=1}^{N_M} \sum_{k=1}^{N_R} P[D_H > d | \mathcal{S}, M = m_j, R = r_k] P[M = m_j] P[R = r_k] \quad (13)$$

which is of the same form as Equation (7). Thus, a performance-based analysis using a lateral spreading model in which loading is a function of  $M$  and  $R$  is computationally equivalent to a PSHA for lateral spreading displacement. The conditional probability term is evaluated using Equation (6) with  $\sqrt{D_H}$  evaluated using the appropriate values of  $M$ ,  $R$ , and  $\mathcal{S}$ . In this manner, the uncertainty in lateral spreading displacement is effectively attributed to the earthquake loading, which is justifiable in light of the common observation of record-to-record variability of ground motions being much higher than uncertainties in terms such as those used to compute  $\mathcal{S}$ . Extension of the procedure to integrate over uncertainties in  $\mathcal{S}$ , although not pursued in this paper, is straightforward.

### Example – Site-Specific Displacement Evaluation

The performance-based lateral spreading model was implemented into the computer program, EZ-FRISK (Risk Engineering, Inc., Boulder, Colorado) using the attenuation table feature of that program to allow prediction of the variation of  $d | \mathcal{S}$  with  $M$  and  $R$ . In this form, EZ-FRISK was able to compute hazard curves for  $d | \mathcal{S}$  at a particular site. Figure 4 shows a lateral spreading displacement hazard curve for a hypothetical site in Seattle, Washington, USA; the ground slope and SPT profile for this site combine to produce a site parameter value,  $\mathcal{S} = -5.7$ . For this particular site and location, the

72-yr, 224-yr, and 475-yr lateral spreading displacements (corresponding, respectively, to 50%, 20%, and 10% probabilities of exceedance in a 50-yr period) are 0.002 m, 0.64 m, and 1.58 m, respectively.

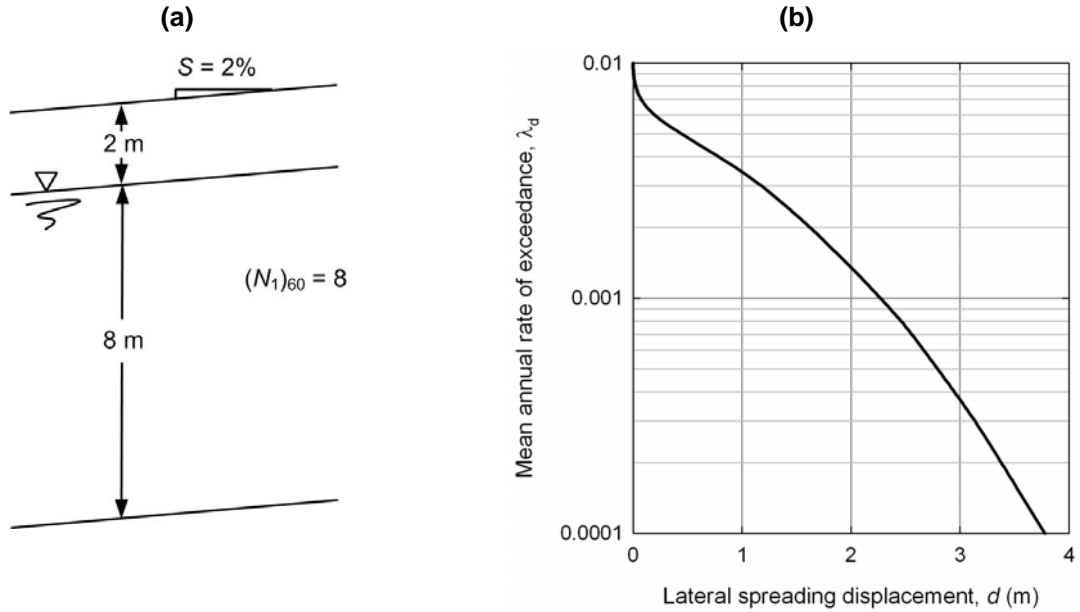


**Figure 4. (a) Hypothetical site in Seattle, Washington (47.53N, 122.30W), and (b) corresponding lateral spreading displacement hazard curve.**

Knowing the mean annual rate of exceedance for a given displacement level, the probability of exceeding that displacement level in a given exposure period,  $T_E$ , can easily be computed as

$$P = 1 - \exp[-\lambda_d T_E] \quad (14)$$

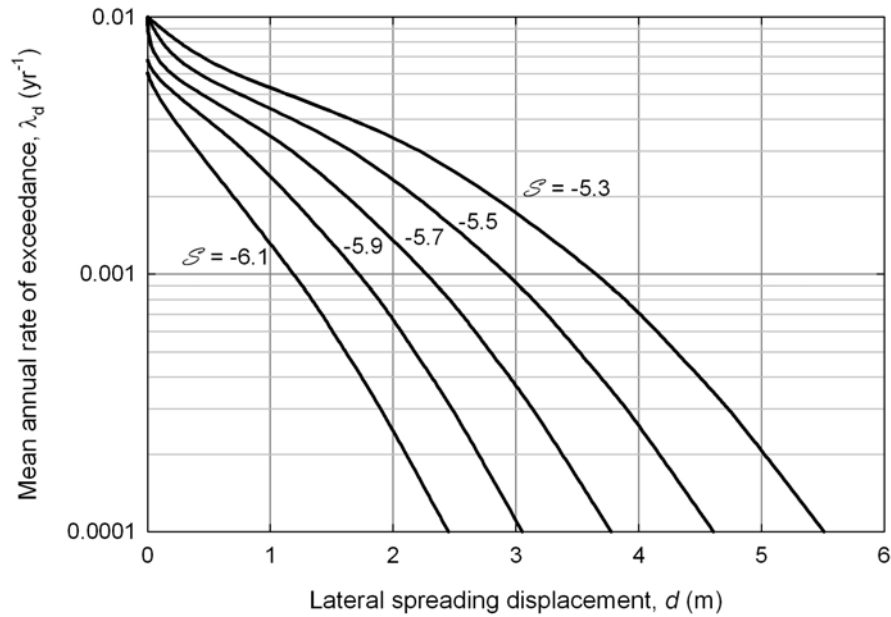
#### *Example – Conditional Displacement Evaluation*

Figure 5 shows a series of conditional hazard curves for different values of  $\mathcal{S}$  at the same Seattle location used to develop Figure 4. Note that a given value of  $\mathcal{S}$  could correspond to many different combinations of  $T_{gs}^*$  and  $S$  or  $T_{ff}^*$  and  $W$ . As previously indicated, the site profile shown in Figure 4(a) corresponds to  $\mathcal{S} = -5.7$ ; increasing the slope of that site to  $S = 4.65\%$  would increase  $\mathcal{S}$  to  $-5.3$ ; the resulting increase in lateral spreading displacement can be read directly from Figure 5. Once the performance-based lateral spreading displacement curves have been computed for a given location, the user is only required to evaluate  $\mathcal{S}$  for the site of interest in order to determine a lateral spreading displacement value with a known mean annual rate of exceedance.

#### *Comparison of Conventional and Performance-Based Evaluations*

In a conventional lateral spreading displacement evaluation, the results of a PSHA are typically used to identify a single scenario on which the evaluation is based. The scenario is defined by deaggregated magnitude-distance pairs – some engineers use mean values of  $M$  and  $R$ , and others prefer to use modal values.





**Figure 5. Hazard curves for conditional lateral spreading displacement for different site term values in Seattle, Washington (47.53N, 122.30W).**

USGS deaggregation analyses for 475-yr peak acceleration values give mean magnitude and distance values of 6.57 and 36.0 km, respectively, for the Seattle site. Corresponding modal magnitude and distance values are 6.64 and 4.0 km, respectively; the large difference in mean and modal distances results from the contributions of the Seattle fault, which runs through Seattle just south of the downtown area.

The median displacement predicted by the Baska (2002) model using the 475-yr mean magnitude and distance values for the site in Figure 4(a) is 1.91 m; using the computed lateral spreading displacement hazard curve for that site, the actual return period for that level of displacement would be 664 yrs. The median displacement using the 475-yr modal magnitude and distance values for the same site is 3.23 m; the lateral spreading displacement hazard curve shows an actual return period of 3867 yrs for that level of displacement. These results indicate the sensitivity of inferred lateral spreading hazard to decisions about how deaggregation results are used; the lateral spreading displacement obtained using modal values is nearly six times less likely to occur than that obtained using mean values.

### *Design Implications*

The performance-based approach can be used to define design criteria in terms of a return period (or return periods) for a given performance objective (or performance objectives). This approach has been shown to produce considerably more uniform and consistent hazards for initiation of liquefaction (e.g. Kramer et al., 2006) due to the fact that all scenarios are considered with appropriate weighting of their relative likelihoods.

If the maximum allowable lateral spreading displacement at the Seattle site was taken to be 1.0 m, the return period of unacceptably large displacement would be about 290 yrs. If the design criterion stated that the minimum return period for unacceptably large displacement was 475 yrs, for example, the curves of Figure 5 show that improvement of the site to conditions corresponding to  $S = -5.9$  would be required. This level of improvement could be achieved by regrading the slope to an inclination of 1.1% (without changing the SPT profile) or by densifying the saturated soils to an SPT resistance of  $(N_1)_{60} = 14.2$  (without changing the slope inclination). The fact that curves of the type shown in Figure 5 can be used to consider the effects of different site geometries and SPT profiles for both ground slope and free-face conditions makes them particularly useful for design purposes.

## SUMMARY AND CONCLUSIONS

This paper has described the development and use of a performance-based procedure for prediction of liquefaction-induced lateral spreading displacements. Commonly used deterministic models for estimation of lateral spreading displacement were reviewed, and the probabilistic model of Baska (2002) introduced. The basic framework of a probabilistic, performance-based lateral spreading displacement analysis was introduced, and the equivalence of that procedure to a PSHA using an alternative formulation of the Baska (2002) model demonstrated. Finally, examples of the use of the performance-based procedure were described.

The results of this work indicate the promise of a performance-based approach to the evaluation of liquefaction-related hazards, such as lateral spreading, and lead to the following general conclusions:

1. Conventional lateral spreading displacement evaluations, which are generally based on a single earthquake scenario, can be quite sensitive to the manner in which that scenario is selected and modelled.
2. It is possible to develop a performance-based approach to lateral spreading displacement evaluation that considers all earthquake scenarios, with the contribution of each to lateral spreading displacement appropriately weighted by relative likelihood.
3. By considering all combinations of earthquake magnitude and distance from all known sources, and also considering the uncertainty in computed lateral spreading displacement given magnitude and distance, the performance-based procedure offers a more complete and, consequently, consistent evaluation of actual lateral spreading displacement hazard than conventional procedures. Any probabilistic lateral spreading model could be used in this framework.
4. Design criteria for lateral spreading could be formulated in terms of displacement levels with specific mean annual rates of exceedance (or return periods). Such criteria would likely produce designs with more consistent levels of risk in different seismic environments than those produced by conventional procedures.

## ACKNOWLEDGEMENTS

The research described in this paper was supported by the Washington State Department of Transportation; the contributions of Tony Allen, Keith Anderson, and Kim Willoughby are gratefully acknowledged.

## REFERENCES

- Ambraseys, N.N. (1988). "Engineering seismology," *Earthquake Engineering and Structural Dynamics*, Vol. 17, pp. 1-105.
- Bardet, J.P. and Seed, R.B., Cetin, K.O., Lettis, W., Rathje, E., Rau, G., and Ural, D. (2000). "Soil liquefaction, landslides, and subsidence," *Earthquake Spectra, The 1999 Kocaeli, Turkey, Earthquake Reconnaissance Report*, Earthquake Engineering Research Institute, 16(A), pp. 141-162.
- Bartlett, S.F. and Youd, T.L. (1992). "Empirical analysis of horizontal ground displacement generated by liquefaction-induced lateral spread," *Technical Report NCEER-92-0021*, National Center for Earthquake Engineering Research, Buffalo, New York.
- Baska, D.A. (2002). "An analytical/empirical model for prediction of lateral spreading displacements," *Ph.D. Dissertation*, University of Washington, Seattle, Washington, 539 pp.

- Boulanger, R.W., Mejia, L.H., and Idriss, I.M. (1997). "Liquefaction at Moss Landing during Loma Prieta earthquake," *Journal of Geotechnical and Geoenvironmental Engineering*, ASCE, 123(5), 453-467.
- Cetin, K.O., Youd, T.L., Seed, R.B., Bray, J.D., Stewart, J.P., Durgunoglu, H.T., Lettis, W., and Yilmaz, M.T. (2004). "Liquefaction-induced lateral spreading at Izmit Bay during the Kocaeli (Izmit)-Turkey earthquake," *Journal of Geotechnical and Geoenvironmental Engineering*, ASCE, 130(12), 1300-1313.
- Comartin, C.D., Greene, M., and Tubbesing, S.K., eds. (1995). "The Hyogo-ken Nanbu Earthquake, January 17, 1995," *Preliminary Reconnaissance Report*, Earthquake Engineering Research Institute, 116 pp.
- Cornell, C.A. and Krawinkler, H. (2000). "Progress and challenges in seismic performance assessment," *PEER News*, April, 1-3.
- Deierlein, G.G., Krawinkler, H., and Cornell, C.A. (2003). "A framework for performance-based earthquake engineering," *Proceedings, 2003 Pacific Conference on Earthquake Engineering*.
- Faris, A., Seed, R.B., Kayen, R.E., and Wu, J. (2006). "A semi-empirical model for the estimation of maximum horizontal displacement due to liquefaction-induced lateral spreading," *Proceedings, 8<sup>th</sup> U.S. National Conference on Earthquake Engineering*, in press.
- Hamada, M., Towhata, I., Yasuda, S., and Isoyama, R. (1987). "Study of permanent ground displacement induced by seismic liquefaction," *Computers and Geotechnics*, Elsevier Applied Science Publishers, 4, 197-220.
- Hamada, M. and Wakamatsu, K. (1998). "Liquefaction-induced ground displacement triggered by quaywall movement," *Soils and Foundations*, Special Issue, 2, 85-95.
- Holzer, T.L., ed. (1998). *The Loma Prieta, California, Earthquake of October 17, 1989—Liquefaction*, U.S. Geological Survey Professional Paper 1551-B, 314 pp.
- Ishihara, K. and Yoshimine, M. (1992). "Evaluation of settlements in sand deposits following liquefaction during earthquakes," *Soils and Foundations*, Vol. 32, No. 1, pp. 173-188.
- Kramer, S.L., Mayfield, R.T., and Anderson, D.G. (2006). "Performance-based liquefaction hazard evaluation: Implications for codes and standards," *Proceedings, Eighth U.S. National Conference on Earthquake Engineering*, San Francisco.
- Krawinkler, H. (2002). "A general approach to seismic performance assessment," *Proceedings, International Conference on Advances and New Challenges in Earthquake Engineering Research*, ICANCEER, 2002, Hong Kong.
- Rauch, A.F. and Martin, J.R. (2000). "EPOLLS model for predicting average displacements on lateral spreads," *Journal of Geotechnical and Geoenvironmental Engineering*, ASCE, 126(4), 360-371.
- Seed, H.B., Lee, K.L., Idriss, I.M., and Makdisi, F. (1973). "Analysis of the slides in the San Fernando dams during the earthquake of Feb. 9, 1971," *Report No. EERC 73-2*, Earthquake Engineering Research Center, University of California, Berkeley, 150 pp.
- Seed, H.B., Lee, K.L., Idriss, I.M., and Makdisi, F. (1975). "The slides in the San Fernando dams during the earthquake of Feb. 9, 1971," *Journal of the Geotechnical Engineering Division*, ASCE, 101(7), 651-688.
- Seed, H.B. (1979). "Soil liquefaction and cyclic mobility evaluation for level ground during earthquakes," *Journal of Geotechnical Engineering*, ASCE, 105(2), 201-255.
- Shamoto, Y., Zhang, J.-M., and Tokimatsu, K. (1998). "Methods for evaluating residual post-liquefaction ground settlement and horizontal displacement," *Soils and Foundations*, Special Issue No. 2, 69-83.
- Youd, T.L. and Perkins, D.M. (1987). "Mapping of Liquefaction Severity Index," *Journal of Geotechnical Engineering*, ASCE, Vol. 113, No. 11, pp. 1374-1392.

- Youd, T.L., Hansen, C.M., and Bartlett, S.F. (2002). "Revised multilinear regression equations for prediction of lateral spread displacement", *Journal of Geotechnical and Geoenvironmental Engineering*, ASCE, 128(12), 1007-1017.
- Zhang, G., Robertson, P.K., and Brachman, R.W.I. (2004). "Estimating liquefaction-induced lateral displacements using the standard penetration test or cone penetration test," *Journal of Geotechnical and Geoenvironmental Engineering*, ASCE, 130(8), 861-871.